



Hydration of cementitious materials, present and future

Karen L. Scrivener^{a,*}, André Nonat^b

^a LMC; IMX, Station 12, EPFL, 1015 Lausanne, Switzerland

^b Institut Carnot de Bourgogne, UMR 5209 CNRS-Université de Bourgogne, 9 Av. A. Savary, BP 47 870, F-21078 Dijon Cedex, France

ARTICLE INFO

Article history:

Received 28 March 2011

Accepted 31 March 2011

Keywords:

Hydration (A)

Kinetics (A)

Ca₃SiO₅ (D)

Portland Cement (D)

ABSTRACT

This paper is a keynote presentation from the 13th International Congress on the Chemistry of Cement. It discusses the underlying principles of hydration and recent evidence for the mechanisms governing this process in both Portland cements and other cementitious materials. Given the overriding imperative to improve the sustainability of cementitious materials, routes to reducing CO₂ emissions are discussed and the impact of supplementary materials on hydration considered.

© 2011 Elsevier Ltd. All rights reserved.

Contents

1. Introduction and scope	651
1.1. Overview on routes to improving sustainability of cementitious materials	652
2. Thermodynamic principles of hydration	653
2.1. Rate of hydration	654
3. Initial dissolution and nucleation	655
3.1. Hydration of C ₃ S	655
3.2. Early reactions of aluminates phases	656
3.3. Onset of acceleration of C ₃ S hydration	657
4. Main hydration peak (acceleration and deceleration periods)	658
4.2. Diffusion control	658
4.3. Space filling (hydrate growth) as a rate controlling mechanism	659
4.4. Hydration beyond 24 h	660
5. Rates of reaction of the different clinker minerals	660
6. Reaction rates of supplementary cementitious materials	661
7. Perspectives on microstructure: structure of C–S–H	662
8. Concluding remarks	664
Acknowledgements	664
References	664

1. Introduction and scope

Hydration is absolutely central to cementitious materials. It is the, almost magical, process by which a fluid suspension is transformed into a rigid solid, at room temperature, without the need for heat or other external processing agents and with minimal bulk volume change. We take it for granted, but just think if we had no previous experience of hydration and someone invented it how sensational that would be!

Because it is so central to the formation and property development of cementitious systems it is critical to understand the underlying mechanisms in order to progress; particularly on the most burning challenge facing the world today—the need to continually lower environmental impact, to do more with less. More specifically, better knowledge of the mechanisms governing hydration can, for example, lead the way to the incorporation of higher amounts of supplementary cementitious materials or to the development of new clinkers. For this reason we try in this paper not only to give a perspective on the current knowledge on the hydration of Portland cement, but of that of other reactive phases and, in addition, to discuss our knowledge of the impact of supplementary cementitious materials on hydration.

* Corresponding author. Tel.: +41 21 6935843.

E-mail address: karen.scrivener@epfl.ch (K.L. Scrivener).

A companion paper for this conference and some other recent reviews, have exhaustively covered the latest publications in this field so we try to avoid covering the same ground. Rather we have chosen to discuss a few generic aspects of the hydration process and highlight progress and outstanding questions relating to the underlying mechanisms.

1.1. Overview on routes to improving sustainability of cementitious materials

The range of practical hydraulic materials is not that large. It is quite surprising to realise that the 8 most common elements in the earth's crust—oxygen (49.4%), silicon (25.8%), aluminium (7.57%), iron (4.7%), calcium (3.39%), sodium (2.64%), potassium (2.4%) and magnesium (1.94%), constitute around 98% of this crust. For materials which are used in such enormous quantities as cement, there is little point in ranging outside this list (with the exception of hydrogen (as water); carbon (in calcites) and possibly sulphur (as sulphate)). Under the highly alkaline conditions found in cements, and critical to the protection of reinforcing steel, iron and magnesium have very low mobility and the alkali metals are highly soluble so largely remain in solution.

Within these oxides the most well known reactive phases are the calcium silicate phases— C_3S and C_2S . In addition to these, Portland cement also contains the aluminate phase C_3A and the ferrite phase $C_2(A,F)$. Apart from these phases, there is really only one other group of hydraulic phases in the system of the most abundant earth oxides—the more alumina rich calcium aluminate which includes CA and $C_{12}A_7$ found in calcium aluminate cements; and $C_4A_3\$$ (equivalent to $3CA + C\$$) found in calcium sulfo aluminate cements and $C_{11}A_7 \cdot CF_2$ found in various rapid setting cements. In the context of reducing CO_2 emissions it is interesting to consider the weight percentage of calcium oxide in these phases, as shown in Table 1. In cementitious materials nearly all sources of lime (CaO) come directly or indirectly from limestone $CaCO_3$ and so the lime content has a direct bearing on the associated emission of CO_2 . It can be seen from Table 1 that the difference in CaO content between C_3S and C_2S is relatively modest, about 10%. Considering the much slower hydration rate of C_2S , which as will be discussed later, seems to be inhibited in the presence of C_3S , even more reactive forms of belite are unlikely to reach 90% of the performance of alite at reasonable hydration times. On the other hand it is clear that the calcium aluminate group of phases can provide a significant reduction in CO_2 emissions. We can take this analysis further by considering the amount of CO_2 emitted per volume of hydrate produced (which is a rough estimate of the capacity to fill porosity and develop strength), as shown in Table 1.

Increasingly the relatively energy intensive and high CO_2 emitting cementitious phases are now replaced by a range of supplementary cementitious materials. With the exception of fine limestone, these are silico-aluminate materials with lower calcium contents than Portland cement, extending along a silica to alumina ratio of about 2 as shown in Fig. 1 (from [1]). Even the best known of these—blast furnace slag and fly ash are in fact available in much smaller quantities than the amount of Portland cement produced and are not available in all locations. Consequently higher levels of replacement can only be achieved on a widespread basis if a much wider range of SCMs, such as

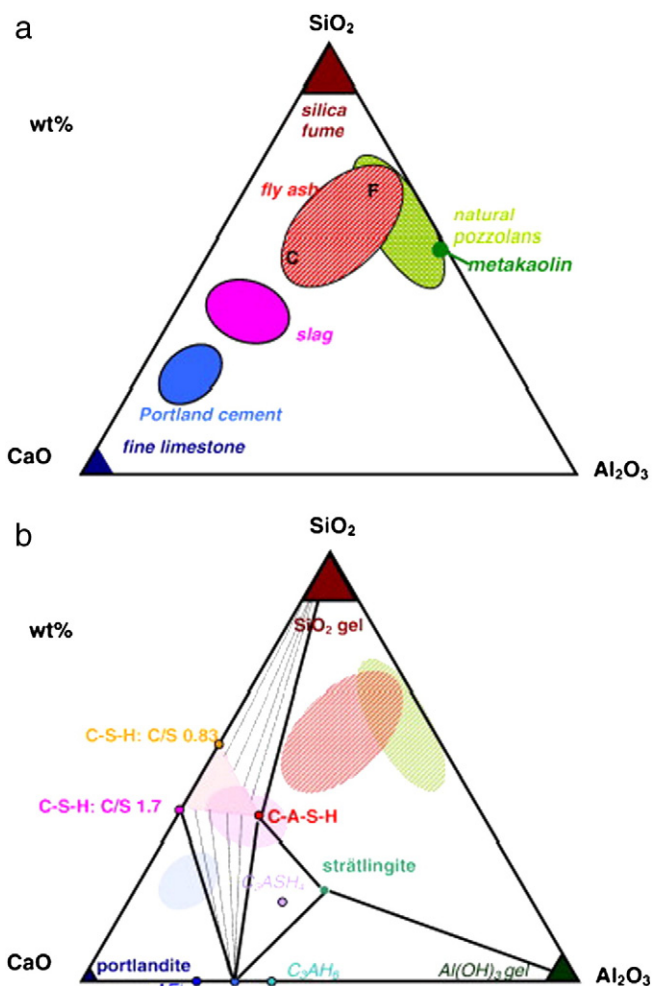


Fig. 1. a) CaO – Al_2O_3 – SiO_2 ternary diagram of cementitious materials, b) hydrate phases in the CaO – Al_2O_3 – SiO_2 system. Note that in the absence of carbonate or sulphate, C_3AH_6 will be more stable than the AFm phases.

natural pozzolans and activated clays, are used. Fine limestone is a particularly interesting SCM, due to its very low cost and near zero associated CO_2 emissions. It is now clear that this can react with calcium aluminates to give space filling calcium carbo-aluminates [2,3].

The relative cost of transport for such a voluminous, cheap material as cement, means that sustainability will necessitate the use of locally available materials. The variability of local materials, particularly SCMs is a major challenge. For these reasons sustainability can only be achieved through an ability to use a wide range of different cementitious combinations adapted to the materials locally available and the application. In the future we need to see:

- increasing use of known SCMs
- development and use of new SCMs
- development and use of different clinker types.

This requires a science based approach to understanding the reactions and performance of such material combinations. However, most developments of cementitious materials have been more or less empirical and incremental. The reasons are probably multiple; the complexity of cementitious materials with many reacting species is certainly an obstacle, but look at the incredible detailed knowledge that has been obtained in living organisms, which are certainly much, much more complex (and of more interest to most people). Therefore, we must also admit that it has been difficult to attract scientists to study these low cost materials and this is not helped by the conservative

Table 1

	wt% CaO	Anhydrous (CO_2 g/g)	Hydrates (CO_2 g/cm ³)
C_3S	74	0.58	0.86
C_2S	65	0.51	0.77
CA	35	0.28	0.48
$C_4A_3\$$	37	0.21 ^a	0.39

^a Assuming 1 mol CaO comes from anhydrite ($CaSO_4$, rather than $CaCO_3$).

nature of the industry, where structures are expected to last in the order of one hundred years with little or no maintenance.

Today, the tide is beginning to turn. With the pressure to reduce greenhouse gas emissions, the industry has realised that more fundamental understanding is needed. Furthermore, with the knowledge of the well established basic concepts of physics and chemistry and the progress of recent years in analytical techniques and modelling, we probably have most of what we need to face these challenges.

Coming back to the theme of this paper, hydration corresponds to the formation of new compounds from the interaction of a cementitious material with water. Improving or developing new cementitious systems requires answers to the following questions:

- What compounds are formed? This is dictated by thermodynamics.
- At what rate? Kinetics depend both on thermodynamics and the specific properties of the anhydrous and hydrated materials (size, morphology, crystallography, defects....).
- How do the hydration products fill in the available space between the anhydrous grains? This determines the final microstructure and then the properties.

Considering potential cementitious materials, we now know the phases which will be produced on reaction with water—Fig. 1. Furthermore, reliable geochemical codes and databases are now available to predict quantitatively the thermodynamically stable phase assemblages which will form for any degree of hydration of any combination of materials and it has been shown that the experimentally found assemblages agree well with these predictions [1,4]. Extensive knowledge exists on the limits of solid solution of the various hydrates although some further work is needed to reliably predict the extent of aluminate substitution in C–S–H. (The topic of thermodynamic modelling is well reviewed in a companion paper for this conference [5]). The area where knowledge is really lacking is in our knowledge of the mechanisms governing the kinetics of reaction of these materials with water.

2. Thermodynamic principles of hydration

It is now absolutely clear that hydration is fundamentally a dissolution–precipitation process. One hundred years ago at the first Chemistry of Cement Conference in London [6] the debate raged between the advocates of a “through solution” mechanism, championed by Le Chatelier, and the solid state theory proposed by others. Since that time, our knowledge of the crystal structures of the anhydrous and hydrate phases make it clear that one cannot transform to the other without the passage of ions through solution. Similarly the dissolution of all the anhydrous phases we consider here must be globally congruent as charge balance and crystal structure would prevent the extensive dissolution of certain species without others. In addition, analysis of the solution during hydration shows unambiguously that this is the path taken in systems which have been studied in detail. (A possible exception to these statements is free lime, which can “hydrate”—react chemically with water at very low relative humidities.)

As a consequence, for hydration to proceed the potential hydration product(s) must have a lower solubility than the anhydrous phase(s). It is clearly illustrated in the simple case of calcium silicates by considering the projection on the $[\text{SiO}_2]$ $[\text{CaO}]$ plane of the CaO – SiO_2 – H_2O phase diagram (Fig. 2).

When the concentration of calcium hydroxide is between 0 and 36 mmol/L (which corresponds to the maximum of supersaturation with respect to portlandite), C–S–H is always less soluble than tricalcium silicate—so C_3S always hydrates. This is also true for silica (amorphous or crystallised) if the calcium hydroxide is greater than 4 mmol/L. On the contrary wollastonite is always less soluble than C–S–H and never hydrates. In the case of C_2S , C–S–H is less soluble at low lime concen-

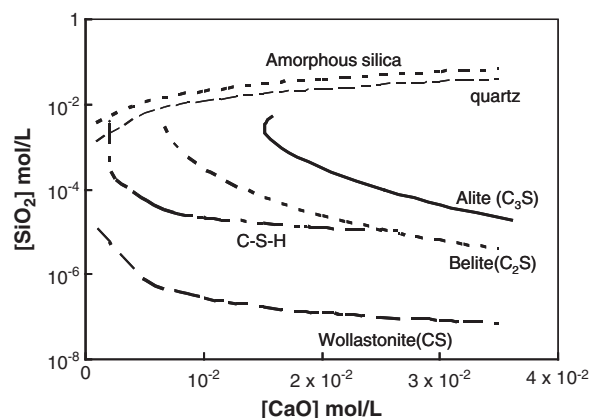


Fig. 2. The solubility curves of silica (amorphous and quartz) and anhydrous calcium silicates (wollastonite, beta dicalcium silicate, and tricalcium silicate) are compared to the solubility of C–S–H.

tration but could be more soluble at high lime concentration (above about 30 mmol/L). Then C_2S should not dissolve to precipitate C–S–H.

The case of the CaO – Al_2O_3 – H_2O system is also interesting to consider because of the existence of several hydrates less soluble than the anhydrous phases. According to the solubility diagram presented in Fig. 3[7], the least soluble phase is C_3AH_6 . But the formation of C_3AH_6 is slower than those of C_2AH_8 or C_4AH_{13} which are more soluble, so the latter two are formed first. Increasing temperature accelerates the formation of C_3AH_6 (see for example a recent publication [8]). This is a good example of the necessary combination of thermodynamics and kinetics to predict the formation of phases.

This kind of approach could be applied to SCMs as well, but is a bit more difficult to visualise easily because there are more than 2 independent variables: Ca, Si, Al, pH and possibly sulphate and carbonate. Reliable geochemical codes are available to calculate the stable phase assemblages. However, the databases need to be completed. The first step should be to determine the solubility of these materials in the relevant solutions if not known. The other point is to improve the modelling of the incorporation of Al in C–S–H in such systems. These are the object of ongoing studies.

However it is useful to keep in mind that the above condition stating the difference of solubility between the anhydrous and the hydrated phase is necessary but not enough in a multiphase system: the best example is the mix of C_3S and C_2S . Both are more soluble than C–S–H, so, in a well mixed system, without local variations, C_2S cannot dissolve as long as C_3S hydrates, because the solution concentrations maintained during the hydration of C_3S are higher than the solubility of C_2S (Fig. 4) [9].

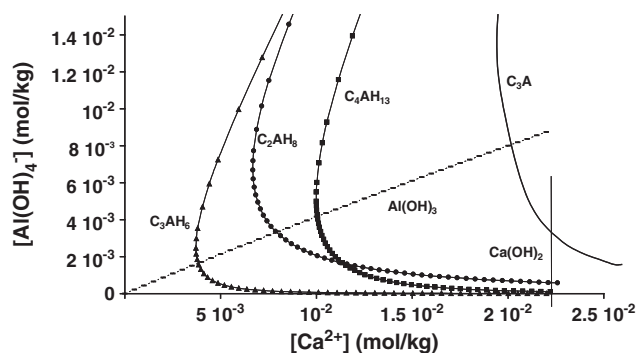


Fig. 3. Solubility curves of the hydrated phases in the CaO – Al_2O_3 – H_2O system. The solubility of C_3A is arbitrary plotted, the solubility product is not well known. From [7].

2.1. Rate of hydration

Hydration is a heterogeneous process: there are at least two solid phases concerned (but most of the time there are more); the initial (anhydrous) and final (hydrated) phases, and one liquid phase. The initial phase dissolves with a dissolution rate R_{diss} , and the final phase precipitates with a precipitation rate R_{prec} . Such heterogeneous reactions are interfacial reactions. Also the rate depends on S , the area of the interface between the solid and the solution.

From a thermodynamic point of view, the greater the departure from equilibrium i.e. the higher ΔG in absolute value, the higher the rates of dissolution and precipitation. Moreover some ions in solution might have a specific effect on the surface reactions. In the case of an isotropic material, the rate of dissolution or precipitation may be written as

$$R(t) = r_{interface}(\Delta G(t), [ions]...)S(t) \text{ (mol.s}^{-1}\text{)}$$

where $r_{interface}$ is the interfacial rate of dissolution or precipitation ($\text{mol.m}^{-2}.\text{s}^{-1}$), $S(t)$ is the area of the dissolving or growing surface (m^2).

Both $r_{interface}$ and S vary with time. Obviously, during the dissolution, the surface decreases because the material is consumed and during precipitation the surface increases. The interfacial rates, $r_{interface}$, of dissolution and precipitation also vary during the hydration process. Indeed, during most of the hydration process, the rate of precipitation is roughly equal to the rate of dissolution because the latter gives the material for the former: $R_{prec} \cong R_{diss}$. Because at the beginning $S_{prec} = 0$ and at the end $S_{diss} = 0$, to satisfy $R_{prec} \cong R_{diss}$, r_{diss}/r_{prec} must continuously increase. This is achieved by the evolution of the concentration of constitutive ions in solution: at the beginning the concentration approaches the solubility of the initial phase, $\Delta G_{diss} \rightarrow \Delta G_{0\text{ diss}}$, $r_{diss} \rightarrow 0$ and ΔG_{prec} is maximum; at the end the concentration is close to the solubility of the final phase $\Delta G_{prec} \rightarrow \Delta G_{0\text{ prec}}$, $r_{prec} \rightarrow 0$ and ΔG_{diss} is maximum. This process is illustrated in the simplest case in Fig. 5. The path followed by the concentrations in solution was named kinetic path by Barret [10].

The beginning of the hydration is always peculiar because, except in the case of seeding, the hydrated phase is not yet present. Consequently there is always a period during which the anhydrous phase dissolves alone to produce enough material into solution to induce the apparition of the new less soluble phase, the precipitate. Indeed, if the formation of

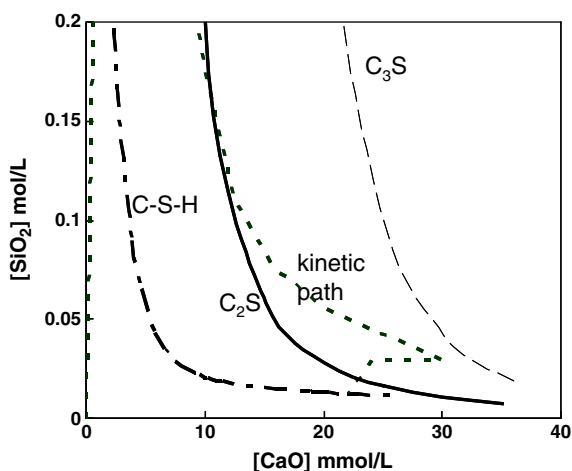


Fig. 4. Relative positions of the solubility curves of C_3S , C_2S and $C-S-H$ in the $CaO-SiO_2$ system. Because of the stoichiometry difference between C_3S and $C-S-H$, during hydration of C_3S , the concentrations in solution follow the dotted curve (kinetic path according to Barret [10]). During most of the process these concentrations are higher than the solubility of C_2S which cannot dissolve in these conditions.

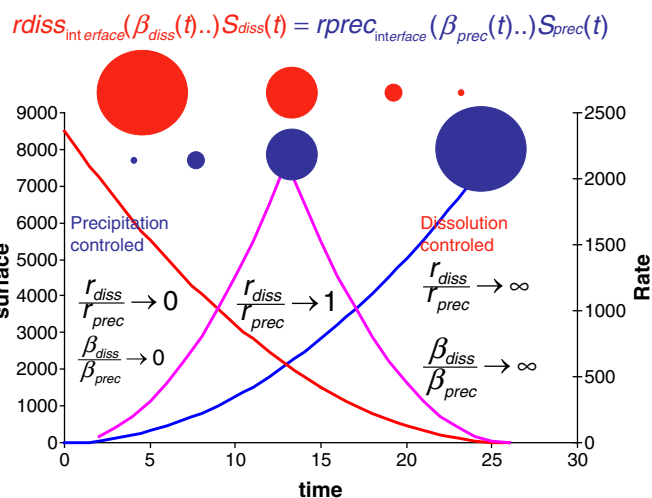


Fig. 5. This picture illustrates the dissolution-precipitation process in an ideal case; a spherical anhydrous particle dissolves to produce a hydrated spherical particle in the bulk solution. The surface of the dissolving particle decreases continuously and the surface of the hydrated particle increases continuously with the same law. For the equation to be satisfied, the dissolution interfacial rate must decrease and the interfacial precipitation rate must increase. This is achieved by the variations of the under and supersaturation respectively. The macroscopic hydration rate is at the maximum when the dissolving and precipitating surfaces are equal.

a less soluble phase decreases the free energy and is favourable, it requires the creation of an interface between the new solid and the solution which requires energy, $S\gamma$, where S is the extent of the interface and γ is the crystal-solution interfacial energy. The excess of energy needed to form the interface comes from the supersaturation of the solution with respect to the precipitating phase. According to the classical nucleation theory, the induction time (t_{ind}) needed to have stable nuclei able to grow depends on the supersaturation β ($=$ (ionic activity product)/(equilibrium solubility product, K_{sp})) and the crystal-solution interfacial energy γ :

$$\ln t_{ind} = \frac{f\Omega^2\gamma^3}{kT(kT)^2 \ln^2\beta} - \ln K_0$$

where f is a form factor, Ω the molar volume, k the Boltzmann constant, T the temperature and K_0 a kinetic constant.

The higher the supersaturation, the shorter the induction time. A high supersaturation will be reached more rapidly if the rate of dissolution of the anhydrous phase is high and if it is much more soluble than the hydrated one. This is the case of the nucleation of $C-S-H$ from the hydration of pure C_3S : the nucleation time is so short it cannot be measured [11]. On the contrary, in the case of hydration of C_2S in lime solution, a nucleation time of several tens of minutes is required to observe the nucleation of $C-S-H$ [4,5]. This time can be even longer in the case of the nucleation of CAH_{10} during the hydration of CA [12,13].

The second parameter, the crystal-solution interfacial energy, γ may also be important. This is the case, for example, during the hydration of a $C_3A-CaSO_4$ mix. The dissolution of this mix gives a solution supersaturated with respect to different phases, ettringite, hydroxy-AFm and monosulphate. Even if ettringite is the most stable phase in these conditions (the least soluble), hydroxy-AFm precipitates before ettringite if $CaSO_4$ is added as gypsum because the interfacial energy of hydroxyl-AFm is extremely small. Increasing the $CaSO_4$ concentration by using calcium sulphate hemi-hydrate which is 4 times more soluble than gypsum (respectively 60 mM and 15.6 mM at 25 °C) significantly increases the supersaturation with respect to ettringite and less with respect to hydroxy-AFm and leads directly to the nucleation of ettringite [14].

In light of these general principles, it is possible to identify what must be taken into account to understand and predict the time

evolution of new and more and more complex cementitious systems. This is the object of modelling. In most of the cases, approximations must be made, but at least the 1st order parameters must not be neglected.

As stated above, during most of the hydration process the following equation is satisfied:

$$R(t) = r_{\text{interface diss}}(t)S_{\text{diss}}(t) = r_{\text{interface prec}}(t)S_{\text{prec}}(t).$$

All the terms of this equation are time dependent; $r_{\text{interface}}(t)$ depends on the “chemistry”, $S(t)$ depends on “geometry”. The evolution of both surfaces, the dissolving phase and the growing phase, over time must be taken into account properly in models. Concerning dissolution, the relative surface of small particles is much greater than coarse ones. In cements, the range of particle sizes is very large ($> \approx 10^3$), and must be explicitly taken into account in a relevant model. It is still more critical and complicated in the case of precipitation; the ideal case presented in Fig. 5 is far from what occurs during hydration of cements: a spherical growth of the hydrates far from the surface of the anhydrous grains is not realistic. Most hydration products grow in an anisotropic way, the anisotropy depending on the crystal structure and chemistry of solution. This is the case of ettringite and C–S–H. It is also well known that C–S–H grows mostly from the surface of the anhydrous grains, into the space between the grains (outer product) and in the space made free by the dissolution (inner product). This also obviously impacts the dissolution interface. Furthermore, we have to keep in mind that a hydrating cement paste, especially in the case of blended cements, is very heterogeneous: the chemistry at the interfaces between the solution and an alite grain or a silica fume particle is very different, and of course, the laws governing the growth rate of hydrates will be different.

It clearly appears, even in a simple case, that a model must take into account a lot of parameters and to be predictive these parameters must be related to the physics and chemistry of the system rather than simply fitting empirical data. Until now most of the proposed models are limited to the case of the hydration of C_3S . None of them is perfect probably because, depending on the type of algorithmic chosen, it is not possible to take into account all the aspects.

3. Initial dissolution and nucleation

3.1. Hydration of C_3S

As it is the major phase in Portland cement, research has focused on the mechanisms governing the hydration of this phase. This phase was also the major subject of a recent summit on cement hydration¹ leading to two significant reviews (one on mechanisms [15] and one on modelling [16]) which discuss in detail studies since the publication of the chapter of Gartner et al. [17] in 2002. The overall pattern of reaction is extremely well known (Fig. 6). One of the most important characteristics is the rapid slow down in reaction after the addition of water leading to a period of slow reaction, before the rate increases again rapidly. This, so called induction or dormant period, is of great practical importance as it provides a time in which concrete can be transported and placed before setting. However, it usually appears just as a minimum in the rate of reaction curve, as in Fig. 6 (taken from real results), rather than a distinct flat period as often shown in texts. This “induction period” has been the subject of much debate and we will not reiterate all the various theories put forward here. For a long while the most widely accepted theory has been that

on the addition of water a thin layer of hydrate forms on the surface of the grains, which inhibits their further reaction. Despite the fact that this seems to give an intuitively reasonable explanation for the observations, there are several important problems with it:

- Despite the very sophisticated imaging techniques now available, there are no direct observations of such a layer. On the contrary, as reviewed in [18], many images show etch pits formed on the surface of cement grains, whose sharp edges make the presence of a barrier layer unlikely (even on wet specimens by AFM [19] (shown as Fig. 17 in [18])).
- It is widely agreed that that first precipitate is a calcium silicate hydrate. However, it is clear that the atomic structure of C–S–H differs radically from that of C_3S and it is very difficult to imagine how such a material could form a virtually impermeable barrier over the surface. C–S–H does precipitate very early on, but appears as isolated clumps on an otherwise smooth or pitted surface (Fig. 7) [20].

Both authors of this paper share the opinion that the initial product formed does not provide a barrier which causes the slowdown of the rate of reaction. Instead, it can be explained according to the basic principles outlined above. Examination of recent literature from the field of geochemistry shows that a slow dissolution period after an initial rapid reaction with water is the norm, rather than the exception for complex ionic-covalent minerals. Most of us are familiar with the idea that a liquid does not solidify exactly at its equilibrium melting point or precipitate exactly at equilibrium saturation. There always occurs a degree of undercooling or oversaturation to provide the extra energy to form the surface of the first nucleus, as discussed above. In an analogous way dissolution from an atomically smooth surface requires extra energy to form the first pit. This explains the typical dissolution behaviour for minerals, shown in Fig. 8a[21], in which the rate of dissolution (plotted on the negative y axis as the inverse of growth) increases downwards on the vertical axis and the degree of undersaturation decreases toward the equilibrium solubility going left to right on the horizontal axis. At high undersaturation, such as occurs on addition of water, the rate of dissolution is high, as the undersaturation provides the extra energy to form etch pits on the surface. Above a certain threshold the rate of dissolution slows dramatically as there is no longer enough energy available to form etch pits and dissolution can only take place by step retreat from existing defects. The energy for etch pit formation is related to the Burger's vector of defects in the crystal. Although the nature of defects in cementitious phases has not been well characterised, the complex nature of the crystal structure and large unit cell means that this will be large. In a recent publication, Juilland et al. [18] show how this dissolution approach can provide a reasonable explanation for the large amount of data available in the literature. The theory is also supported by experimental results of Nicoleau and Nonat [22] (Fig. 9) which shows a similar curve to that derived from the interpretation of calorimetry results by Kumar and Scrivener [23] (Fig. 8b). As soon as C_3S is in contact with water it dissolves, calcium, silicate and hydroxide concentrations increase in solution, decreasing the degree of undersaturation and so the rate. Knowing the evolution of these concentrations with time, it is possible to calculate the evolution of the undersaturation with time and then the rate (Fig. 10). Fig. 10b shows a quasi instantaneous strong decrease of the rate which corresponds to the first peak measured by calorimetry (this is broadened by the time delay of most calorimeters).

This theory can also explain the annealing experiments on alite leading to a much longer induction period [18]. The role of crystallographic defects was already studied during the 70s principally by Fierens and Verhaegen [24], but the role of dissolution on the early hydration process was not put forward at this stage.

Maybe not all details of the dissolution theory are yet clear. For example, in a discussion of the paper by Juilland et al., Gartner [25]

¹ The International Summit on Cement Hydration Kinetics and Modeling was held on July 27, 28 and 29, 2009 at Laval University, Quebec, Quebec City, Canada. A selection of articles from this conference will be published as a special issue of CCR in 2011.

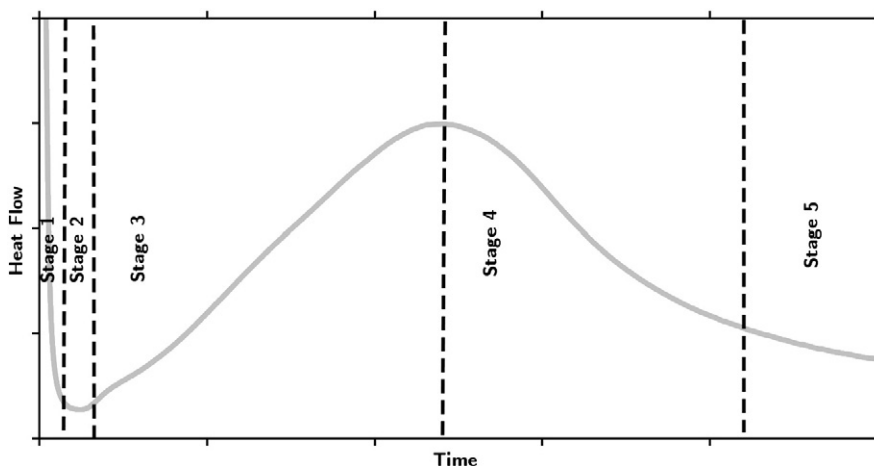


Fig. 6. Rate of heat evolution during hydration of alite, ($w/c = 0.4$). Stages 1 and 2, slow down in dissolution and induction period; stage 3 acceleration period, stage 4 deceleration period, stage 5 slow ongoing hydration.

questioned the very large difference between the concentration of the solution when the dissolution rate slows down and the equilibrium solubility of C_3S calculated from bulk thermodynamics, compared to the difference seen in other minerals. A partial explanation for this may be that the true solubility of alite (which cannot be measured due to the rapid precipitation of products), is determined by its surface, which in water has a structure markedly different from the bulk, or that in vacuum. It is a semantic question, whether a hydrolysed surface should be considered as a separate phase or not.

3.2. Early reactions of aluminate phases

Without sulphate the aluminate (and ferrite) phase reacts rapidly leading to flash set. For this reason calcium sulphate is always added to Portland cement clinkers during grinding. The reaction is slowed down and the essential period of workability is regained. In fact the overall pattern for reaction of C_3A with gypsum is similar to that of C_3S ; with an initial rapid reaction quickly slowing down followed by a period of slow reaction, before the rate again increases. Many text books attribute the slowdown in reaction in the presence of calcium sulphate to the formation of a barrier of ettringite around the grains. If we consider the morphology of ettringite crystals it is apparent that the idea of these forming a barrier is even more absurd than for C–S–H—imagine trying to construct a water tight layer with sticks. Over 25 years ago Scrivener

[26] showed pictures of C_3A hydration where it was clear that the ettringite crystals form out in solution and in no sense form a barrier around the grains. The layer of product directly in contact with the grain (at the time, proposed to be amorphous) was more recently shown to be

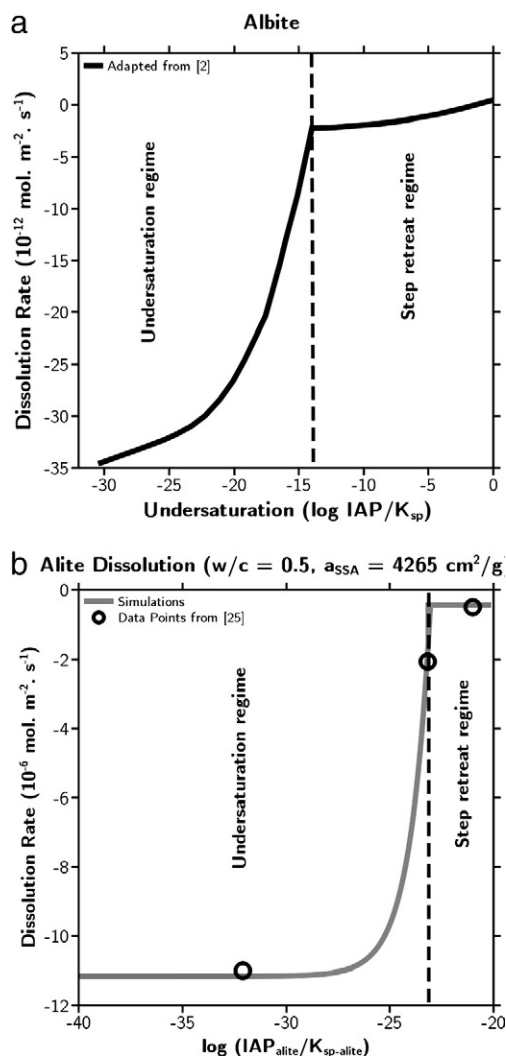


Fig. 8. Dissolution profiles versus undersaturation for (a) Albite (adapted from [20]) and (b) Alite (as obtained from simulations for $w/c = 0.5$ and $a_{ssa} = 4265 \text{ cm}^2/\text{g}$). The round symbols represent measured values from [25].

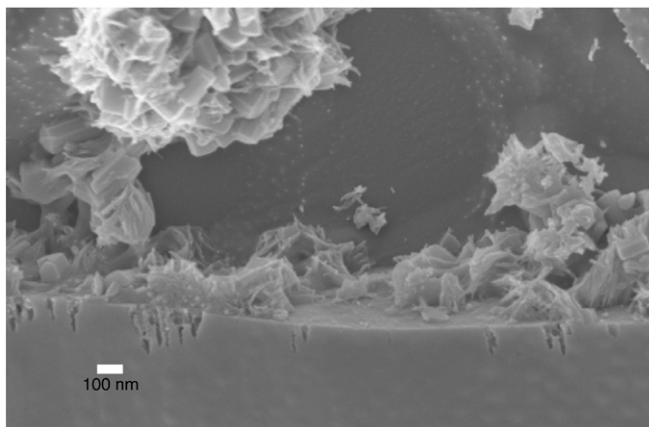


Fig. 7. Morphology Portland cement hydrated for 360 min as observed in the cryo SEM. The sample has fractured through an alite grain. Hydration products, C–S–H and ettringite can be seen deposited on the surface of the grain, but not covering it and many areas of the surface are free of products. The fracture through the grain clearly reveals the etch pits formed on the alite grain surface. Image from Luc Nicoleau of BASF [20].

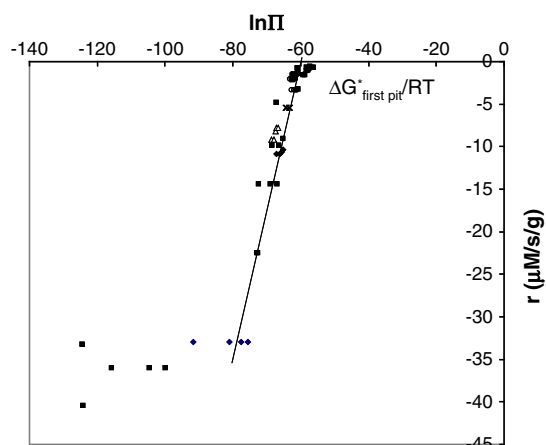


Fig. 9. Rate of dissolution of C_3S (triclinic modification) in function of $\text{Log}(\Pi)$ measured in stirred diluted suspensions. The water/ C_3S ratio is chosen in a way that the solution remains undersaturated with respect to C–S–H ($W/C=10,000$ and $50,000$). $\Pi = (Ca^{2+})^3(H_4SiO_4)(OH^-)^6$ is the activity product. Since $\Delta_{diss}G = \Delta_{diss}G^0 + RT \ln \Pi$, the intercept with the x axis could be considered as $\ln k$ where k is the solubility constant of C_3S superficially hydroxylated; it is difficult to extrapolate here. On the contrary, the intercept of the slope of the decreasing part of the rate would be the free energy of the formation of the first pit. From [21].

a hydroxyl AFm phase by Minard et al. [27], who also showed it was present in systems with calcium sulphate as well as those without. For this reason this AFm phase cannot be the cause of the slowdown of the reaction either and furthermore, there is less of the AFm phase formed when C_3A is hydrated with hemihydrate instead of gypsum, whereas the reaction slows down faster. Another argument, is that the reaction becomes faster (the second peak) when ettringite is still present, but when all the sulphate ions in solution are consumed.

Taking this evidence into consideration, it is clear that, as proposed by Minard et al. [27], the reaction of C_3A must be slowed down directly by absorption of sulphate ions on reactive sites. This effect of

ions on the dissolution of mineral is not unique to C_3A , it is also a general behaviour. In the same manner that some ions can inhibit the growth of crystals, some can slow down the dissolution; it is for example the case of phosphates on the dissolution of C_3S [28]. It is also interesting to note that this hypothesis is similar to the theory of solution controlled dissolution for alite described above.

Throughout the first stage of the reaction, ettringite continues to form at a slow rate. Detailed analysis of the kinetics show that the rate is linear with time if the changes in surface area according to the particle size distribution are taken into account [27,29]. This, and the rather high activation energy of the process [29], again supports the idea of dissolution control.

A further example of a reacting phase showing an induction period without the formation of a barrier layer is Calcium Aluminate Cement, CAC [12]. In this case the concentrations of calcium and alumina in solution both increase to quite high levels and again the rate of dissolution drops to a low rate.

In the light of the clear evidence that most reactive cementitious phases do not produce barrier layers, the question is why alite should be the only exception to this. The success of the solution controlled dissolution theory in allowing the impact of various parameters on the induction period of alite to be quantitatively modelled [23] provides further support to this theory.

3.3. Onset of acceleration of C_3S hydration

The mechanism causing the acceleration of hydration is still not agreed. This is because at this point two events occur almost simultaneously for the hydration of C_3S in a small amount of solution (in paste):

- precipitation of calcium hydroxide (Portlandite)
- rapid growth of C–S–H.

Many theories have been proposed based on both these occurrences and have been considered in detail in recent reviews [15,17]. For a long time the role of the precipitation of portlandite was dismissed as the key mechanism, due to the fact that the addition of this phase can retard hydration. However, in the light of the theory of solution controlled dissolution of alite described above, such experiments can be reassessed: small additions of calcium hydroxide do not act as seeds since they quickly dissolve upon initial contact with water, so the solution undersaturation is decreased with respect to the anhydrous phases. As a result, the rate of dissolution of the anhydrous silicate phases will decrease. Therefore, even though the system is rapidly saturated with lime early on, the slow dissolution rate imposed by the reduction in the undersaturation will lead to a delay before the acceleration period.

When the volume of the solution is increased (higher w/c), because the portlandite is much more soluble than C–S–H, a greater amount of C_3S must dissolve to precipitate CH. In these conditions, calcium hydroxide always precipitates after the acceleration and so, is not its origin (Fig. 11). It is also possible to fully hydrate C_3S without any calcium hydroxide precipitation by maintaining the lime concentration below the critical supersaturation [30].

However, the portlandite precipitation decreases the calcium hydroxide concentration and increases the undersaturation with respect to C_3S and so contributes to increasing the rate of reaction (Fig. 11[31]).

The hydration accelerates for the reasons explained above (Fig. 5). The initial dissolution of C_3S leads to a solution supersaturated with respect to C–S–H which precipitates. The number of nuclei formed in the first minutes depends on the rate of dissolution, the volume of the solution and the initial concentration of the solution. As these nuclei grow, the surface of precipitation defined above, S_{prec} increases and so does the rate. It has been shown that the higher the number of nuclei, the faster the hydration [32]. It is also known that seeding the mix

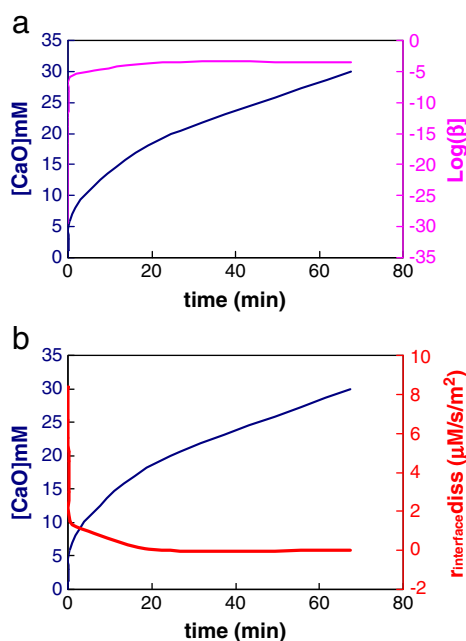


Fig. 10. (a) Evolution of the degree of undersaturation with respect C_3S during the beginning of hydration according to the strong increase of the calcium hydroxide concentration. (b) Calculated rate of dissolution of C_3S according to the variation of undersaturation represented in (a).

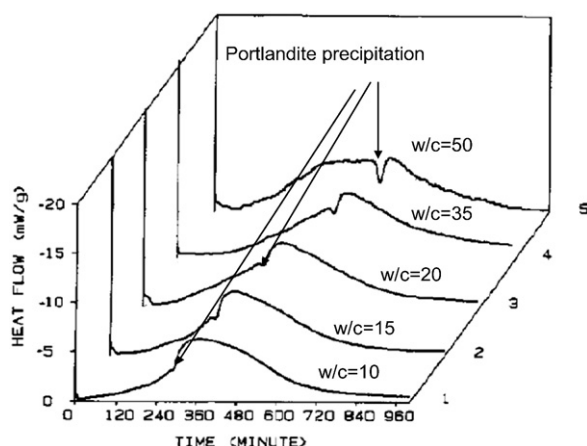


Fig. 11. Heat evolution rate curves for the C_3S hydration in lime saturated solutions with a different solution to C_3S ratios. The portlandite precipitation revealed by an endothermal peak in the curve, occurs later and later when the w/c increases. From [31].

with C–S–H accelerates the reaction. This principle has been recently used to develop new accelerators [33]. A seeding experiment performed by Thomas et al. [34] also shows that the acceleration period occurs much earlier in the presence of C–S–H seeds. Such experiments clearly indicate that the onset of the acceleration period corresponds to the onset of rapid growth of C–S–H. It seems that a certain extent of dissolution is needed in order to provide the stable nuclei that will trigger the acceleration period. From this perspective, the dissolution mechanisms would be the rate limiting factor that could explain the presence of an apparent induction period when no stable seed is present initially.

As discussed in the next section, the growth of C–S–H, is a significant rate limiting factor during the acceleration period, which is more gradual and prolonged than in other cementitious systems (for example, calcium aluminate cements and ettringite forming systems, including calcium sulpho aluminate cements and CAC plus gypsum).

There is some evidence that the length of the “induction” period, maybe linked to the presence of Al in solution coming from the dissolution of alite, but also from the aluminate phases in the case of Portland cement [35,36]. An explanation could be that Al ions poison the growth of the C–S–H nuclei formed initially. Because the solution is still supersaturated with respect to C–S–H, C–S–H continues to nucleate but does not grow as long as some Al is available in solution. Once all the Al are adsorbed on C–S–H nuclei, the new Al free C–S–H nuclei can grow and the hydration accelerates in the same way as in the case of pure C_3S . The same behaviour is seen when C_3S is hydrated in a solution containing some Al ions [37].

4. Main hydration peak (acceleration and deceleration periods)

The onset of the acceleration period leads to the main hydration reaction of alite, characterised by a period in which the reaction accelerates to a peak, followed by a period of deceleration. Again it is interesting to note that this pattern of a main reaction peak is followed by most cementitious systems, for example C_3A plus gypsum, calcium aluminate cements and calcium sulfo aluminate cements and plaster. This pattern of reaction is also typical of many metallurgical reactions as considered by Avrami in the 1930s. The well known Avrami equation was derived for the case of homogeneous nucleation of a phase in a finite volume. The rate of reaction is proportional to the surface of the growing phase, which initially increases and then decreases, when the growing regions start to impinge and the free surface area decreases, as shown in Fig. 12.

Experimental evidence indicates that in the hydration of alite the rate of reaction is also proportional to the surface area of the product (Fig. 13 from [38,39]). However, in alite the nucleation of C–S–H seems to occur mainly close to the surface of the alite grains rather than homogeneously as captured by the Avrami equation. A boundary nucleation and growth (BNG) equation may better capture such a situation and was recently shown by Thomas to fit well for the reaction of C_3S [40]. However, although both the Avrami and BNG equations can be fitted to reaction curves of alite and C_3S , the physical meaning of the fit parameters should be closely considered. For example a tremendous range of fit parameters for the Avrami equation can be found in the literature. This comes partly from the fact that the range of particle sizes of the reacting materials is rarely considered in detail. Most ground cementitious phases have a wide range of particle sizes, from less than tenths of a micron to 70 μm or more. Considering typical reaction rates, particles below 1 μm are consumed by about 10 h. As small particles make up a high proportion of the overall surface area of a powder, the consumption of the small particles, will have a major effect on slowing down the rate of the reaction. This factor was the rationale for the coupled experimental/modelling study of hydration made at the EPFL and Dijon in recent years described below. In these and other studies, the acceleration part of the peak, can be captured by modelling the nucleation and growth process. More difficult to identify, and controversial are the mechanisms responsible for the deceleration period.

4.2. Diffusion control

It is useful to consider the evidence for a switch to diffusion control as being the cause of the onset of the deceleration period. Throughout the acceleration period, C–S–H continues to grow around the alite grains, building up a layer around 1 μm in thickness. It is often thought that when this layer of hydration product around the alite grains reaches a certain thickness, the reaction slows down due to the time needed for diffusion through the layer. Another possibility is that the layer of hydrates establishes a concentration gradient and decreases the undersaturation adjacent to the alite grains, which slows down the rate of reaction as discussed before. In either case, one would expect to see similar hydrate layer thicknesses at the peak around alite grains of all sizes, even when these sizes are hydrated separately. This is not the case as shown in Fig. 14, taken from the work of Costoya [41]. The thickness of the hydration layer around small grains is much greater than that around large grains. Because of this if one tries to fit the deceleration period with diffusion control [42] one finds it necessary to change the parameter related to the diffusion coefficient of C–S–H by an order of magnitude across the range of particle sizes studies (6–80 μm). As it is formed through solution, the C–S–H is the same in each case (as confirmed by electron microscopical observation) so it cannot be presumed to have such a widely varying diffusion coefficient.

Further qualitative evidence comes from the fact that in Portland cement, regions of very low density product persist between the hydrating grain and the “shell” of hydrates (so called Hadley grains see for example the recent publication [43]). If diffusion through the shell was limited, these regions would be expected to fill in sooner.

Ultimately the rate of hydration will decrease due to the reduction in surface area of the hydrating particles as illustrated in Fig. 5. An example of this is the case of plaster for which gypsum crystals grow into the solution and do not cover at all the hemi hydrate crystals; however the rate passes by a maximum and decreases only because the amount of remaining hemihydrate is not enough to produce calcium sulphate at the same rate as at the beginning. The case of C_3S is a bit more complicated by the fact that C–S–H precipitates onto the surface of C_3S . It is clear in Fig. 3 that the decrease of the rate after the maximum is linked to a decrease of the surface of C–S–H.

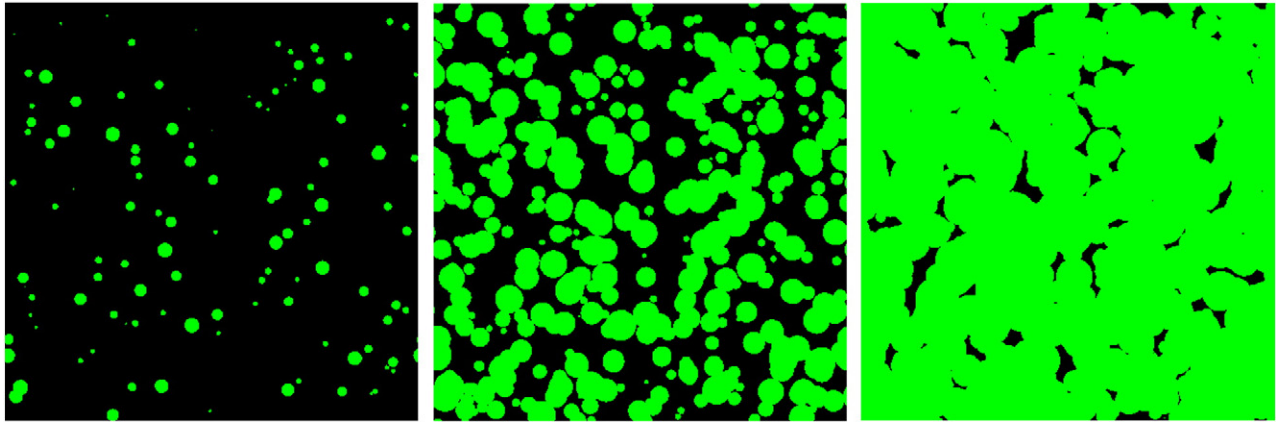


Fig. 12. Homogeneous nucleation and growth as described by the Avrami equation, initially the rate of growth increase as the surface of the precipitates increase. When precipitates start to impinge the rate of growth slows down as the available surface decreases.

4.3. Space filling (hydrate growth) as a rate controlling mechanism

Having eliminated a switch to diffusion control as the cause of the deceleration period, space filling or how hydrate growth fills in the available space—as in the original Avrami case—has to be considered in more detail. Two models have been developed on this idea with different approaches:

The model developed in Dijon is close to the physical process experimentally observed, initial nucleation onto the C_3S surface and anisotropic growth. It works with different particle sizes accounting for the particle size distribution of alite but only with parts of grains and is not able to generate a microstructure. The grains are approximated by spheres constituted by cubic particles of the same size. The C_3S grain surface can be then described by a squared network. The heterogeneous nucleation is modelled by a random distribution of cubic particles [30,32,44,45] on the anhydrous surface. The C–S–H growth is then described by aggregation of new cubic particles around the first ones. This growth or aggregation is anisotropic as suggested by AFM observations [11] and occurs at two different rates parallel and perpendicularly to the grain surface. At each iteration, each cluster on the surface matrix grows parallel to the surface according to the V_x and V_y rates and perpendicularly to the surface according to the perpendicular growth rate V_z . This process increases the surface of C–S–H and then the rate until the growth clusters start to meet which induces a decrease of the C–S–H surface and then of the rate. At this stage, it is considered that the rate of dissolution of C_3S reduces as a concentration gradient builds up through the hydrate layer. The growth continues until complete coverage of the surface. Then, the growth only continues

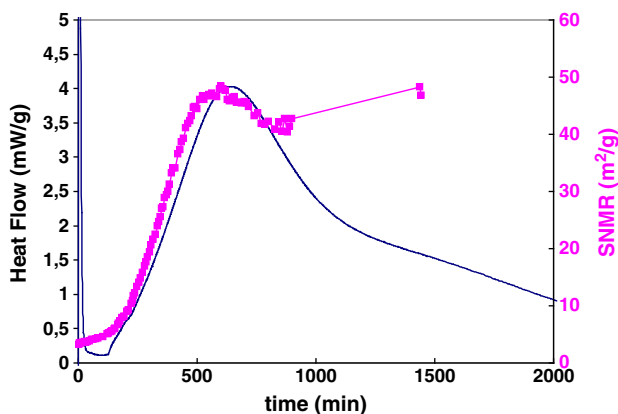


Fig. 13. Correlation with the evolution of the surface of C–S–H in contact with free water and the heat evolution during the hydration of C_3S . The surface is measured from the relaxation time of water by Nuclear Magnetic Relaxation Dispersion. From [38,39].

perpendicularly to the surface until the full C_3S grain consumption and the rate is completely controlled by the rate of dissolution which continuously decreases because of the consumption of the grains as presented in Fig. 5. The input data are the size of the grains which determine the surface of the growth; the parameters are fixed by the

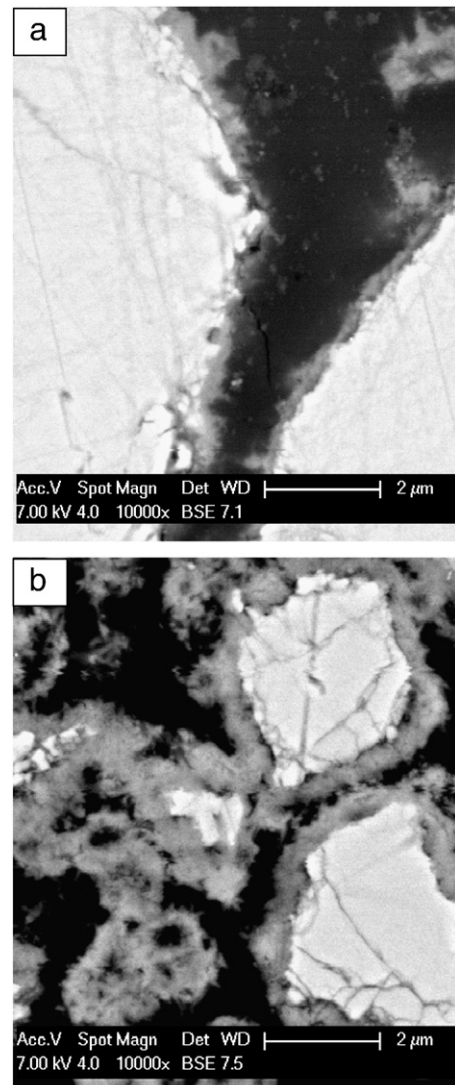


Fig. 14. Images of two sizes of alite particles, hydrates separately, taken near the peak in reaction rate: a) original particle size 38 µm; b) original particle size 6 µm.

chemistry; they are the number of initial nuclei, the parallel growth rate, the perpendicular growth rate and a coefficient describing the permeability of the C–S–H layer formed around the grain. The output data are the degree of hydration over the time, the surface area developed by C–S–H, and the thickness of the C–S–H layer over the time.

The model developed by Bishnoi at EPFL— μic —can consider a large number of particles and their overlaps explicitly to produce a 3D microstructure [42,46]. Particles are represented as spheres, which allows the complete range of particle sizes to be considered—this is typically 2 million particles in a 100 μm box. Kinetics and the arrangement of products can be input by the user to test different hypotheses. When reasonable values for the density of C–S–H are used it is found that the volume of C–S–H at the peak rate of reaction is insufficient to cause impingement with C–S–H growing on neighbouring alite particles and hence a deceleration. However microstructural observations such as in Fig. 15 from Richardson [47], suggest that the effective packing of C–S–H is very far from uniform and the packing density decreases as one moves further from the grain surface. Consequently, it was proposed that, during the early hours of hydration, C–S–H grows in a loosely packed manner and then densifies at later times. Implementation of this hypothesis with μic gave good fits to the experimental data across a range of particle sizes [42]. When integrated with the mechanism whereby the rate of dissolution depends on the undersaturation of the solution (as described in Section 3.1) up to the start of the acceleration period excellent fits to the calorimetric data can be obtained across a wide range of particle sizes for the same parameters Fig. 16[23].

Having seen how a mechanism of space filling can explain the reaction maximum seen in alite, it is interesting to consider other cementitious reactions. A recent study of Gosselin [8] showed that space filling appeared to explain the shape of the main hydration peak in calcium aluminate cements (Fig. 17). In this case the hydration products are crystalline and the rate of growth seems to be very fast. Very steep acceleration periods appear to be generally the case for crystalline hydrates. This suggests that the rate of growth of C–S–H is still very much rate controlling during the acceleration period, leading to the dramatic difference between Fig. 17 and 6.

4.4. Hydration beyond 24 h

In typical cements, without admixtures, the main heat evolution peak is over by 24 h. Typically a normal Portland cement is about 50% hydrated at one day. Up to 28 days the degree of hydration typically increases to around 80% and most of the unhydrated material is the slow reacting belite phase. Over the same time period from 24 h to 28 days the strength of a typical concrete will increase two to four times. Despite the practical importance of this longer term hydration the mechanisms

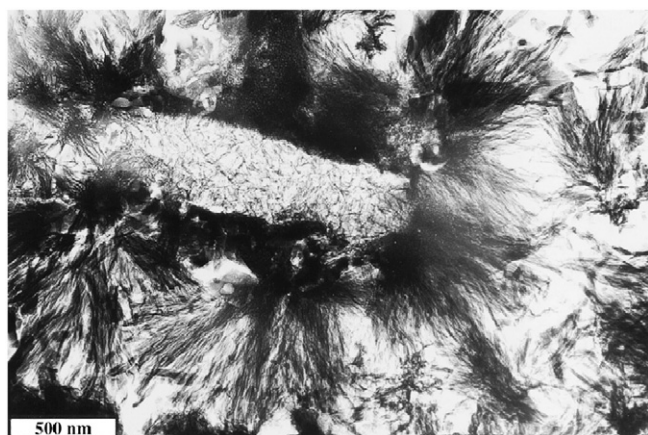


Fig. 15. Transmission electron micrograph showing outer C–S–H with variable “packing density”, generally decreasing with the distance from the grain surface. From [45].

which operate have been much less studied. In 1984 Parrott and Killoh [48] put forward an empirical equation, for the long term reaction.

$$R = K_3(1-D)^{N_3}$$

Where R is the rate or reaction, D the degree of hydration and K_3 and N_3 fitted constants. In their paper they say “preliminary trials suggested that the diffusion equation could not predict the later stages of hydration. Other standard equations were worse than this diffusion equation so the following equation was tried and found to be successful with a range of hydrating materials”. They go on to suggest that this equation is an empirical representation of the formation of a coating around the grains which creates a barrier that slows down the transport of dissolved species. This equation merely captures the fact that the rate goes down as the degree of reaction increases. As discussed above, there are several explanations for such a behaviour, ranging from the reduction in the surface area of reactive phase available (Fig. 5 and exacerbated by the wide PSD), to space filling, so one should be careful in deducing a mechanism from such a general fitted equation. It is clear that there is a need for further study of this reaction period, which includes consideration of all the effects of particle size distribution, product overlap, etc. Experiments performed in diluted suspensions with different size fractions of C_3S by Garrault et al [29] are going in this way. The results after the decelerated period reveal a linear relationship between the rate and S/E where S is the surface area of the grain and E is the thickness of the C–S–H layer formed in agreement with the first Fick law.

5. Rates of reaction of the different clinker minerals

Of course it is well known, that the different clinker phases react at different rates. Studies have generally focussed on the alite and aluminate phases as the most reactive phases. Figs. 18 and 19 present data on the degree of reaction from several literature studies [49–52], and from the work of Kocaba [53] for 4 different cements respectively. The data of Kocaba uses the recent methodology of Rietveld analysis. Despite the variability in the data, as would be expected from different studies on different materials, several general features stand out. Alite and aluminate are confirmed to be the most reactive phases with degrees of reaction of between 40 and 60% for alite and 20–80% for aluminate at 1 day. The data of Kocaba, where the same method is used for all the cements, illustrates that the rate of reaction of aluminate varies significantly between cements, probably due to differences in the microstructure of the interstitial phases and sulphate content.

Perhaps the most striking feature is the data for belite, which clearly shows little reaction (less than 20%) up to 7–10 days. As discussed at the beginning of the paper it seems that the solution concentrations produced by hydrating alite inhibit the dissolution of belite. Such effects are underlined by data on the degree of reaction of belite in slag blends from Kocaba [53], Fig. 20, which shows that the low reaction of belite is prolonged, up to 100 days or more in these systems, probably due to the solution conditions produced by the reacting slag. These results indicate the interest of minimising the belite content in cement to be used with SCMs.

Also of interest are the data for the reactivity of the ferrite phase, this is generally regarded as slowly reacting, but the degree of reaction may not be that much less than the aluminate phase, with around 40% reaction at 1 day in the data of Kocaba. In contrast to belite, it was found by Kocaba that the reaction of ferrite was much enhanced in the presence of slags (Fig. 21), with almost complete reaction after a few weeks. These findings are apparently at odds with microstructural observations, that ferrite regions may be observed even in concrete hydrated for many years (Fig. 22 and [54]). It appears that while the iron oxide constituents remain virtually in the same place, the calcium and alumina contents may be incorporated into hydration products.

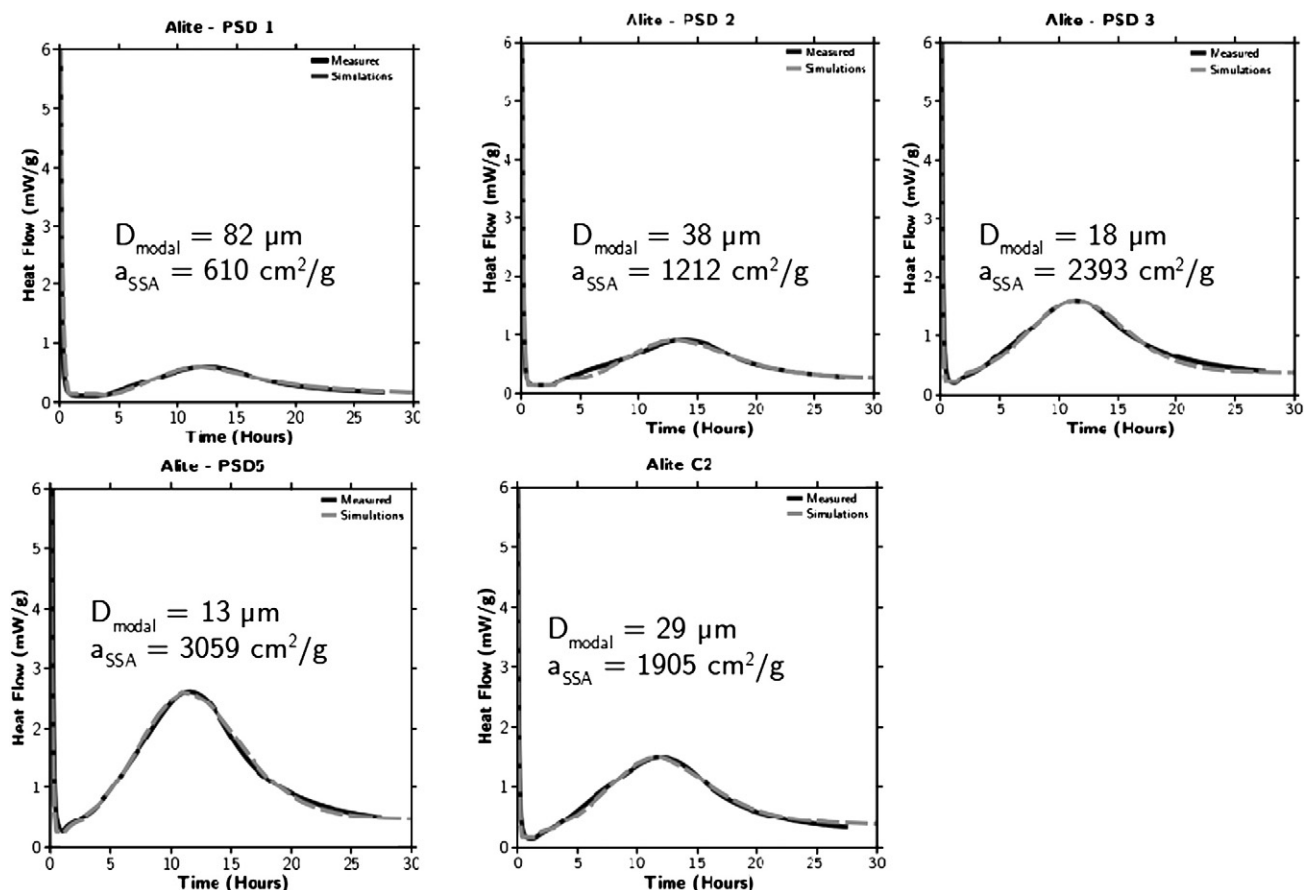


Fig. 16. Experimental and simulated calorimetry curves for a range of particle size distributions of alite, incorporating the mechanisms of solution controlled dissolution (Section 3.1) and nucleation with densifying growth from [23].

6. Reaction rates of supplementary cementitious materials

In the light of the routes towards more sustainable cementitious materials discussed at the beginning of this paper, an understanding of the mechanisms controlling the rate of reaction of SCMs, their interaction with the clinker phases, and the parameters affecting these is clearly of great importance. However our understanding of

these aspects is very much in its infancy and has not yet extended beyond broad generalities. For example it is well accepted that amorphous materials tend to be more reactive than crystalline ones, but even here there are exceptions. Crystalline zeolites (with high internal porosity) react faster than the dense glasses found in slags and fly ashes. It is also well accepted that alkalis increase the rate of reaction of glasses, but such effects are complicated by the negative influence of alkalis on long term strengths.

Within the wide range of amorphous compounds seen in slags and fly ashes, it is generally considered that reactivity increases with increasing calcium content, but again the picture is complicated, due to the fact that fly ashes may contain glasses of several different compositions [55] and that high lime materials, may contain clinker phases such as C_3A .

There are two major obstacles to a better understanding of SCM reactivity:

- Complete characterisation, including reactive surface area and particle size distribution.
- Practical analytical techniques to measure the degree of reaction of the SCMs in blended systems independently of the degree of reaction of cement.

The second point was studied for slags in the recent work of Kocaba [53,56] and is discussed in more detail in [1]. In this study it was found that the most reliable method was the quantification of unreacted slag by image analysis and mapping in the SEM. It was found that the evolution of the degree of reaction of the slags was quite different for the two slags studied, but that the type of Portland cement used seemed to have little impact on the reaction of the slag. It was also found that there was no simple correlation between the degree of reaction of the

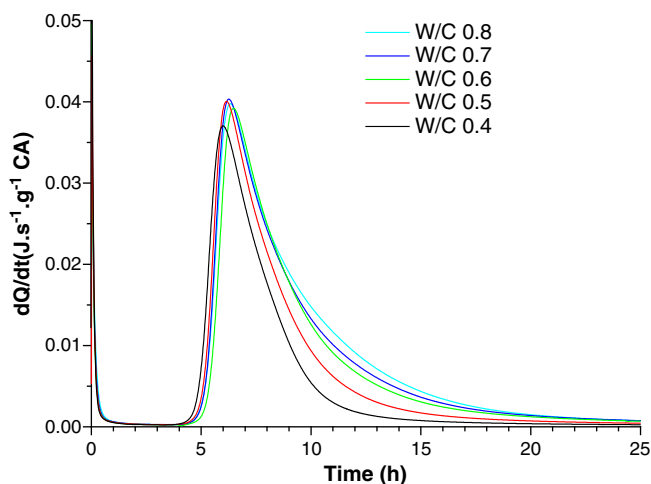


Fig. 17. Effect of w/c on hydration of CAC, indicating space filling as the dominant mechanism for the deceleration part of the reaction. From [8].

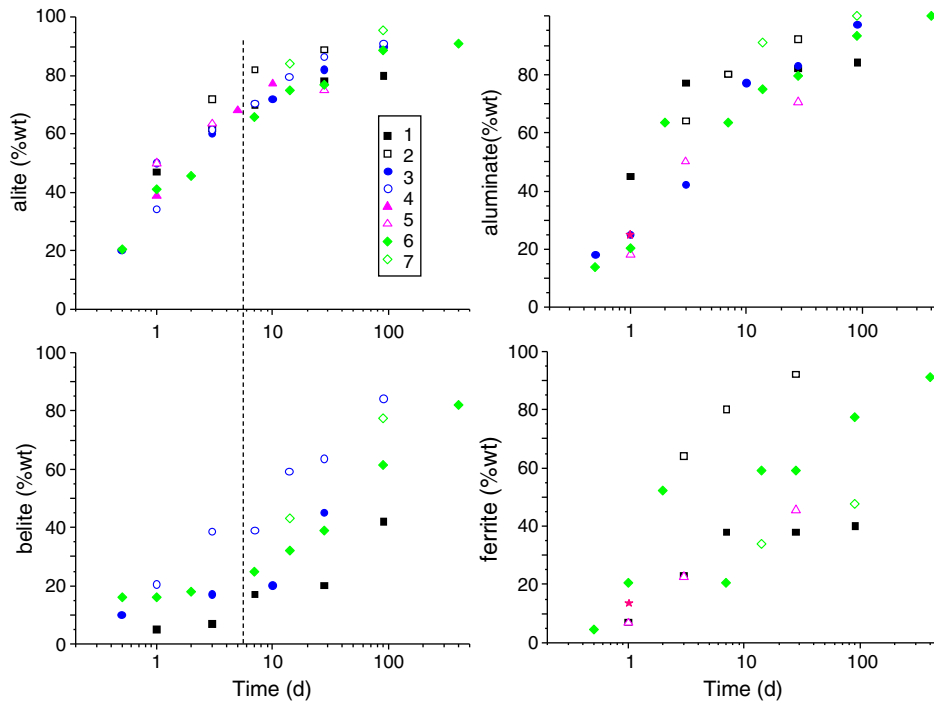


Fig. 18. Degree of reaction of major clinker phases, from literature: 1: Asaga ICCS 92 [46]; 2: Hoshino JAdvConcr06 [47]; 3: Gutteridge CCR90 [48]; 4–7: Taylor, Cement Chemistry [49].

materials and the gain in strength. As strength gain is the most widely reported measure in the literature this underlines the difficulties in understanding the reactivity of SCMs.

Furthermore, a recent NMR study of the hydration of a CEM V tends to show that the silicate and the aluminate parts of the slag do not react at the same rate, the aluminate part reacting much more rapidly [57].

7. Perspectives on microstructure: structure of C–S–H

The basic elements of the microstructural development of cement paste and concrete have been well described previously (e.g. [26,58]). The biggest challenge for the future is to be able to predict properties directly from the microstructure. Despite some promising studies [e.g. 59,60], progress in deriving properties from microstructure has been

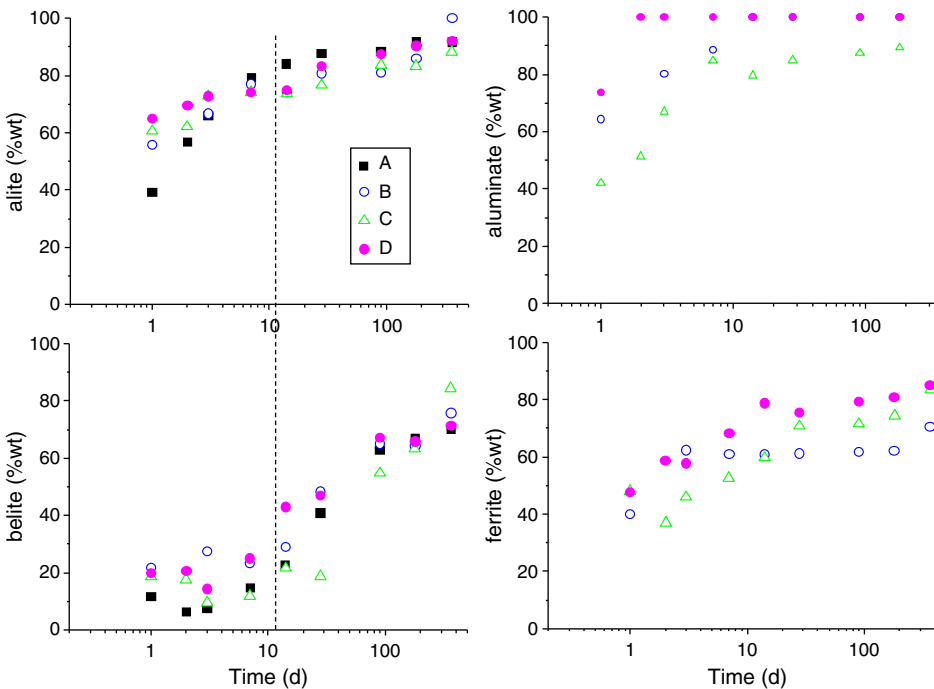


Fig. 19. Degree of reaction of the major clinker phases, from Kocaba [50] for 4 different Portland cements.

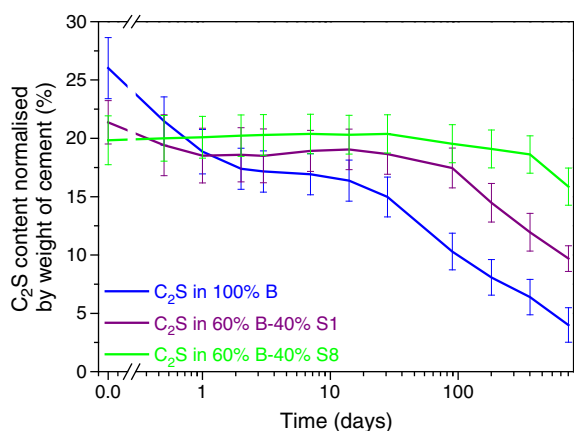


Fig. 20. Reaction of belite in pure Portland cement and in slag cement blends. From [50].

slow, especially at the cement paste level. This is mainly due to the problems of bridging length scales. The representative volume element (RVE), is generally regarded as being 3–5 multiples of the largest feature, so for cement paste this would be around 200–300 μm . At the same time the smallest important features are well below 0.1 μm in size.

This challenge is made more difficult by the complex and variable nature of C–S–H. The potential impact of C–S–H is highlighted by the apparent anomalies in the relation of properties to porosity seen in blends with SCMs. As illustrated by the thermodynamic calculations in [1], additions of SCM result in a lower overall total of hydrate volume at full hydration. In spite of this it is well accepted, and demonstrated by hundreds of studies, that the long term strength and transport properties of such blends are usually superior to those of plain Portland cement. This is usually explained by a “refinement” of the pore structure as measured by Mercury Intrusion Porosimetry. Recent publications from Richardson and co-workers [61,62] have highlighted the very significant differences between C–S–H formed in plain Portland cements and that formed in blends with SCMs, such as slag. While the former has a “fibrillar” appearance (Fig. 15), the latter appears more “foil” like (Fig. 23). These differences in morphology may partially explain such “refinement” and improved properties in blended materials.

The micrographs of Richardson also highlight the ongoing debate about the “meso” structure of C–S–H (in the 1–500 nm range). These fibrillar and foil-like morphologies result from the difference of C–S–H growth depending on the conditions (rate of precipitation, ionic

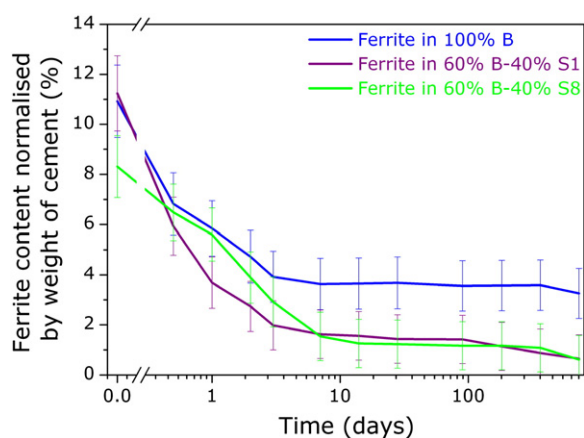


Fig. 21. Impact of slag on the reaction of the ferrite phase. From [50].

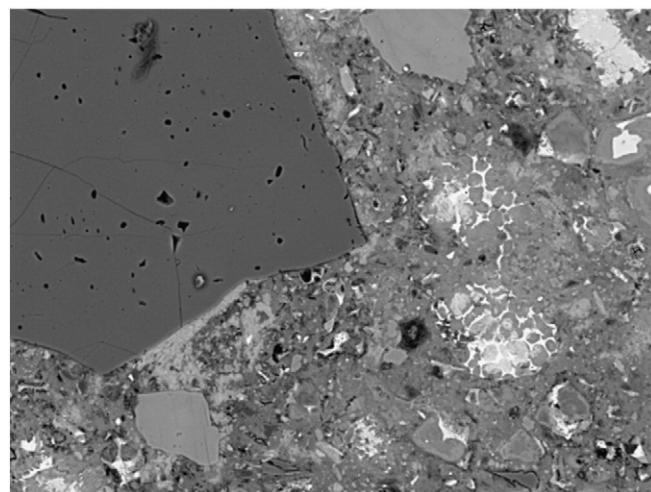


Fig. 22. Microstructure of concrete from building, approximately 30 years old. The original cement is almost completely reacted. The cores of some belite grains remain and the regions originally of ferrite phase can still be identified by their white colour. However, as discussed in the text, these regions are almost certainly reacted to leave the iron oxide component in place.

concentrations, available space....). Despite the general agreement that C–S–H is nanocrystalline in the sense that small local regions (5–30 nm in size), have a layer structure based on a defective tobermorite, the way in which these regions are arranged together to give a more or less dense material and the reasons why, is not understood yet. Some experimental work suggest a granular nature of C–S–H [e.g. 63–68]. The question at issue is whether such region are discrete as suggested by Allen et al. [69], or linked by layers which continue from one nanocrystalline region to another, as in semicrystalline polymers. From a mechanical point of view, both models may show “granular” behaviour, if the links between the nanocrystalline regions are much weaker than the regions themselves.

Other interesting information has come from the use of proton NMR to study the water movement and porosity in cementitious materials. One of the most important aspects of this technique is that it can probe porosity in completely saturated materials, which have never been dried. A series of publications by McDonald and co-

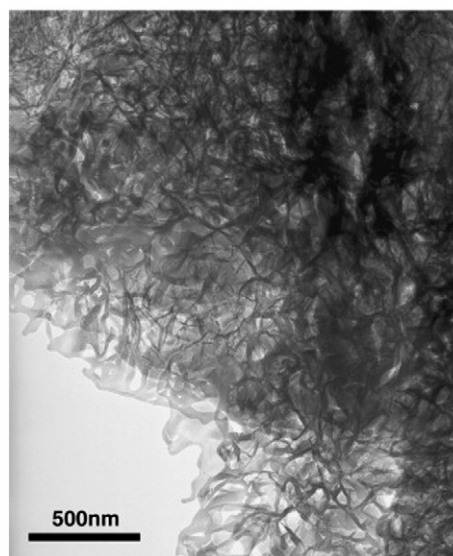


Fig. 23. Foil like C–S–H. From [59].

workers [70–73] indicates that there are two distinct populations of pores (roughly 2–5 and 14–30 nm in size), both of which seem to be associated with the C–S–H, Fig. 24 [74]. It is currently suggested [73] that the smaller size is associated with water between the layers of C–S–H and the larger size with “pore” between the noncrystalline regions.

In the coming years atomistic scale modelling will have a major role to play in advancing our understanding of cementitious materials. A recent publication by Pellenq et al. [75] makes a major contribution to understanding the nanocrystalline regions of C–S–H. Despite some controversy about the distribution of silicate polymers in this model, the approach seems very promising.

8. Concluding remarks

In this paper we have tried to emphasise that hydration obeys well established principles of chemical thermodynamics and kinetics and how our quantitative understanding of the underlying mechanisms is now starting to advance rapidly. This is an example of the type of science based approach which is essential if we are to master the increasingly diverse range of cementitious materials needed to improve sustainability.

In particular we emphasise the following points:

- The slowdown in the initial reaction of C_3S /alite can be explained simply by the changes in concentration in solution, without the need to invoke the presence inhibiting layers blocking reaction. In this respect it behaves like other minerals and other cementitious phases. (However, from a thermodynamic standpoint the surface of alite and other phases in contact with water may be quite different from their bulk structures).
- The growth of C–S–H controls the acceleration period and the growth of this phase appears to be slower compared to crystalline hydrates, which form in other cementitious materials. There may be possibilities to manipulate this growth and accelerate strength development.

- The reasons for the slowdown in reaction after about 10 h are still not totally clear, but we need to think beyond the simplistic idea of a layer of hydrate slowing reaction. Reduction in the available surface area and local changes in concentration at the surface of the grain, may play a role. Also in pastes it seems that space filling plays an important role.
- The mechanisms governing on-going hydration beyond the first day are not yet well clarified, despite their importance for long term properties.
- Studies of the rates of reaction of the different clinker phases indicate a delay in the reaction of belite due to the presence of alite, which is further exacerbated by the presence of slag.
- An important area for future study is a better understanding of the factors controlling the rate of reaction of SCMs. Such studies are opened up by new analytical techniques to quantify the reaction of SCMs independently of the clinker phases.
- Another important feature related to SCMs is the understanding of the changes which occur in C–S–H and the influence of this and other microstructural changes on properties of these materials.

We are optimistic that the next 4 years until the following ICC, will be very rich in progress in quantitative and predictive understanding of hydration and microstructural development. Models at all levels will play an important role, from those at a microstructural level, to those at the atomistic scale.

Acknowledgements

KS would like to thank the Swiss National Science Foundation, who has made the main contribution to funding of our research; AN thanks CNRS, the Regional Council of Bourgogne and ATILH for financial support. Many of our colleagues in the Nanocem network, have greatly contributed to the ideas presented in this paper and to funding our research. More importantly thanks are due to Emmanuel Gallucci, Sandrine Gauffinet, Danièle Perrey and many students whose PhD work has been quoted from—Mercedes Costoya, Shashank Bishnoi, Vanessa Kocaba, Alexandra Quennoz, Patrick Juilland, Aditya Kumar, Denis Damidot, Xavier Lecoq, Jean-Philippe Perez, Luc Nicoleau, Hélène Minard, Yannick Sallier and Maciej Zajac.

References

- [1] B. Lothenbach, K. Scrivener, R.D. Hooton, Supplementary cementitious materials, Review Article Cement and Concrete Research 41 (3) (2011) 217–229.
- [2] T. Matschei, B. Lothenbach, F.P. Glasser, The role of calcium carbonate in cement, Cement and Concrete Research 37 (4) (2007) 551–558.
- [3] B. Lothenbach, G. Le Saout, E. Gallucci, K. Scrivener, Influence of limestone on the hydration of Portland cements, Cement and Concrete Research 38 (6) (2008) 848–860.
- [4] B. Lothenbach, F. Winnefeld, Thermodynamic modelling of the hydration of Portland, Cement and Concrete Research 36 (2) (2006) 209–226.
- [5] D. Damidot, B. Lothenbach, D. Herfort, F.P. Glasser, Thermodynamics and cement science, Cement and Concrete Research 41 (7) (2011) 679–695 (this issue).
- [6] The setting of Cements and Plasters: A General Discussion, Transactions of the Faraday Society effectively the 1st conference in the series which became the International Conferences on the Chemistry of cement, Vol 14, 1919, pp. 1–46. <http://pubs.rsc.org/en/journals/journalissues/tf>.
- [7] J. Perez, Etude de l'hydratation des phases constitutives d'un ciment Portland et de la résistance mécanique des pâtes pures et mortiers : Influence des trialcenolamines, PhD Thesis, Université de Bourgogne, 2002.
- [8] C. Gosselin, E. Gallucci, K. Scrivener, Influence of self heating and Li_2SO_4 addition on the microstructural development of calcium aluminate cement, Cement and Concrete Research 40 (10) (2010) 1555–1570.
- [9] Calculated from data in ref 10.
- [10] P. Barret, D. Bertrandie, Fundamental hydration kinetic features of the major cement constituents: Ca_3SiO_5 and bCa_2SiO_4 , Journal de Chimie Physique 83 (11/12) (1986) 765–775.
- [11] S. Garraut-Gauffinet, A. Nonat, Experimental investigation of calcium silicate hydrate (C–S–H) nucleation, Journal of Crystal Growth 200 (3–4) (1999) 565–574.
- [12] P. Barret, D. Bertrandie, Hydration of aluminate cement, Advances in Cement and Concrete. Proceedings of an Engineering Foundation Conference, July 24–29, 1994, Durham, NH.

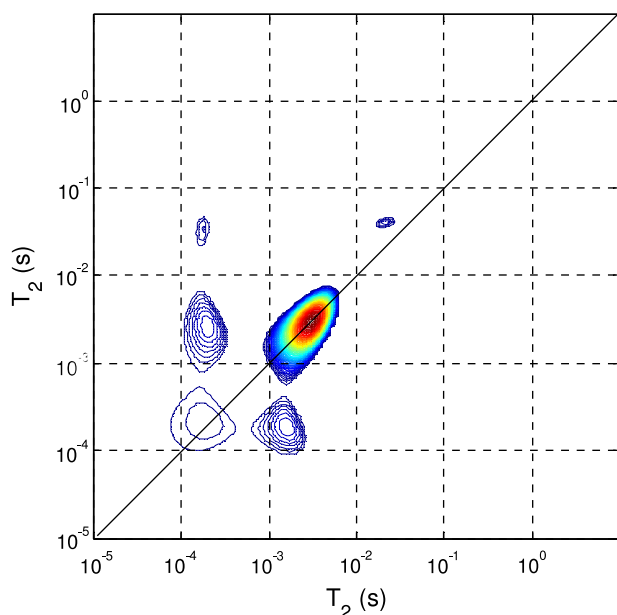


Fig. 24. Results from a 1H NMR experiment [75]; white cement at 1 day. The different regions (peaks, with intensity shown in colour) along the diagonal indicate two distinct populations of pores in C–S–H. The regions with the shortest T_2 relaxation time ($\approx 10^{-4}$ s) are the smallest pores in size (2–5 nm) thought to be water within C–S–H nanocrystalline regions. The next population ($T_2 \approx 10^{-3}$ – 10^{-2} s) are pores. The off diagonal area indicates the exchange of water between these peaks.

- [13] D. Damidot, D. Sorrentino, D. Guinot, Factors influencing the nucleation and growth of the hydrates in cementitious systems: an experimental approach, in: A. Nonat (Ed.), *Hydration and Setting. Why Does Cement Set? An Interdisciplinary Approach*, Rilem Publications, 1997, pp. 161–197.
- [14] S. Pourchet, et al., Early C₃A hydration in the presence of different kinds of calcium sulfate, *Cement and Concrete Research* 39 (11) (2009) 989–996.
- [15] J.W. Bullard, H.M. Jennings, R.A. Livingston, A. Nonat, G.W. Scherer, J.S. Schweitzer, K.L. Scrivener and J.J. Thomas “Mechanisms of cement hydration”. *Cement and Concrete Research* in press, doi:10.1016/j.cemconres.2010.09.011.
- [16] J.J. Thomas, J.J. Biernacki, J.W. Bullard, S. Bishnoi, J.S. Dolado, G.W. Scherer and A. Lüttge “Modeling and simulation of cement hydration kinetics and microstructure development”, *Cement and Concrete Research* in press, doi:10.1016/j.cemconres.2010.10.004.
- [17] E.M. Gartner, J.F. Young, D.A. Damidot, I. Jawed, Hydration of Portland cement, in: J. Bensted, P. Barnes (Eds.), *Structure and Performance of Cements*, 2nd edition, Spon Press, 2002, pp. 57–103.
- [18] P. Juilland, E. Gallucci, R. Flatt, K. Scrivener, Dissolution theory applied to the induction period in alite hydration, *Cement and Concrete Research* 40 (6) (2010) 831–844.
- [19] Hélène di Murro, “Mécanismes d’élaboration de la microstructure des bétons”, PhD Thesis, Université de Bourgogne, 2007.
- [20] Nicoleau, L. Private communication.
- [21] A.C. Lasaga, A. Lüttge, Variation of crystal dissolution rate based on a dissolution stepwise model, *Science* 291 (2001) 2400–2404.
- [22] L. Nicoleau, D. Perrey and A. Nonat; submitted to *Cement and Concrete Research*.
- [23] A. Kumar and K.L. Scrivener, Modelling early age hydration kinetics of alite, in press, *Cement and Concrete Research*.
- [24] P. Fierens, J.P. Verhaegen, Hydration of tricalcium silicate in paste — kinetics of calcium ions dissolution in the aqueous phase, *Cement and Concrete Research* 6 (1976) 337–342.
- [25] Gartner, E; Discussion of the paper “Dissolution theory applied to the induction period in alite hydration” by P. Juilland et al., *Cement and Concrete Research* 40 (2010) 831–844, *Cement and Concrete Research*, 41 (5) 2011, 560–562.
- [26] K.L. Scrivener, The microstructure of concrete, in: J.P. Skalny (Ed.), *Materials Science of Concrete I*, American Ceramic Society, Columbus, Ohio, 1989, pp. 127–161.
- [27] H. Minard, S. Garrault, L. Regnaud, A. Nonat, Mechanisms and parameters controlling the tricalcium aluminate reactivity in the presence of gypsum, *Cement and Concrete Research* 37 (10) (2007) 1418–1426.
- [28] P. Bénard, et al., Influence of orthophosphate ions on the dissolution of tricalcium silicate, *Cement and Concrete Research* 38 (10) (2008) 1137–1141.
- [29] Quennoz, A. Hydration of C₃A with calcium sulfate alone and in presence of calcium silicate, PhD Thesis, EPFL, 2011.
- [30] A. Nonat, X. Lecoq, S. Gauffinet, Calcium hydroxyde concentration in solution: parameter determining the kinetics of the early hydration of tricalcium silicate and the characteristics of the products, 10th International Congress on the Chemistry of Cement, 1997. Gothenburg, June 2–6, 1997.
- [31] D. Damidot, A. Nonat, C₃S hydration in diluted and stirred suspensions: (I) Study of the two kinetic steps, *Advances in Cement Research* 6 (21) (1994) 27–35.
- [32] S. Garrault, A. Nonat, Hydrated layer formation on tricalcium and dicalcium silicate surfaces: experimental study and numerical simulations, *Langmuir* 17 (26) (2001) 8131–8138.
- [33] Nicoleau, L., New calcium silicate hydrate network. Transportation research record: Journal of the Transportation Research Board, 2142(2010): p. 42–51.
- [34] J.J. Thomas, H.M. Jennings, J.J. Chen, Influence of nucleation seeding on the hydration mechanisms of tricalcium silicate and cement, *Journal of Physical Chemistry C* 113 (11) (2009) 4327–4334.
- [35] Y. Sallier, PhD Thesis, Université de Bourgogne 2008.
- [36] F. Begarin, S. Garrault, A. Nonat, L. Nicoleau, Study of alite containing aluminium hydration, *Annales de Chimie — Science- des Matériaux VOL 33 (Suppl. 1) (2008) 251–258*.
- [37] Begarin Cement and concrete science.
- [38] M. Zajac, PhD Thesis, Université de Bourgogne 2007.
- [39] M. Zajac, et al., Effect of temperature on the development of C–S–H during early hydration of C₃S, in: J.J. Beaudoin, J.M. Makar, L. Raki (Eds.), 12th International Congress on the Chemistry of Cement, 2007, Montreal.
- [40] J.J. Thomas, A new approach to modeling the nucleation and growth kinetics of tricalcium silicate hydration, *J. Am. Ceram. Soc.* 90 (2007) 3282–3288.
- [41] Costoya, M., Kinetics and microstructural investigation on the hydration of tricalcium silicate: PhD Thesis, EPFL, 2008 (<http://library.epfl.ch/theses>)
- [42] S. Bishnoi, K.L. Scrivener, Studying nucleation and growth kinetics of alite hydration using μ ic, *Cement and Concrete Research* 39 (10) (2009) 849–860.
- [43] E. Gallucci, M. Mathur, K. Scrivener, Microstructural development of early age hydration shells around cement grains, *Cement and Concrete Research* 40 (1) (2010) 4–13.
- [44] S. Garrault, T. Behr, A. Nonat, Formation of the CSH layer during early hydration of tricalcium silicate grains with different sizes, *J. Phys. Chem. B* 110 (2006) 270–275.
- [45] S. Garrault, L. Nicoleau, A. Nonat, Tricalcium silicate hydration modeling and numerical simulations, *Proceeding of CONMOD*, 2010, Lausanne.
- [46] S. Bishnoi, K.L. Scrivener, μ ic: a new platform for modelling the hydration of cements, *Cement and Concrete Research* 39 (4) (2009) 266–274.
- [47] I.G. Richardson, The nature of C–S–H in hardened cements, *Cement and Concrete Research* 29 (8) (1999) 1131–1147.
- [48] L.J. Parrot, D.C. Kiloh, Prediction of cement hydration, *Proceedings British ceramic Society*, 35, 1984, pp. 41–54.
- [49] K. Asaga, M. Ishizaki, S. Takahashi, K. Konishi, T. Tsurumi, M. Daimon, Effect of curing temperature on the hydration of Portland cement compounds, *Proceedings 9th International Congress on the Chemistry of Cement*, New Delhi, India, Vol. IV, 1992, pp. 181–187.
- [50] S. Hoshino, K. Yamada, H. Hirao, XRD/Rietveld analysis of the hydration and strength development of slag and limestone blended cement, *Journal of Advanced Concrete Technology* 4 (3) (2006) 357–367.
- [51] W.A. Gutteridge, J.A. Daziel, Filler cement: the effect of the secondary component on the hydration of Portland cement: Part I. A fine non-hydraulic filler, *Cement and Concrete Research* 20 (5) (1990) 778–782.
- [52] H.F.W. Taylor, *Cement Chemistry*, Thomas Telford Publishing, 1997.
- [53] Kocaba, V. Development and evaluation of methods to follow microstructural development of cementitious systems including slags, PhD Thesis EPFL 2010.
- [54] K.L. Scrivener, A study of the microstructure of two old cement pastes, *Proc. 8th Int. Cong. on the Chemistry of Cements*, Vol. III, 1986, pp. 389–393, Rio de Janeiro.
- [55] R.T. Chancey, P. Stutzman, M.C.G. Juenger, D.W. Fowler, Comprehensive phase characterization of crystalline and amorphous phases of a Class F fly ash, *Cement and Concrete Research* 40 (1) (2010) 146–156.
- [56] Kocaba, V., Gallucci, E and Scrivener, K.L. Methods for determination of degree of reaction of slag in blended cement pastes, to be published *Cement and Concrete Research*.
- [57] F. Brunet, et al., Characterization by solid-state NMR and selective dissolution techniques of anhydrous and hydrated CEM V cement pastes, *Cement and Concrete Research*. 40 (2) (2010) 208–219.
- [58] K.L. Scrivener, Backscattered electron imaging of cementitious microstructures: understanding and quantification, *Cement and Concrete Composites* 26 (2004) 935–945.
- [59] E.J. Garboczi, D.P. Bentz, Multiscale analytical/numerical theory of the diffusivity of concrete, *Advanced Cement Based Materials* 8 (2) (1998) 77–88.
- [60] Z.H. Sun, E.J. Garboczi, S.P. Shah, Modeling the elastic properties of concrete composites: experiment, differential effective medium theory, and numerical simulation, *Cement & Concrete Composites* 29 (1) (2007) 22–38.
- [61] R. Taylor, I.G. Richardson, R.M.D. Brydson, Nature of C–S–H in 20 year old neat ordinary Portland cement and 10% Portland cement–90% ground granulated blast furnace slag pastes, *Advances In Applied Ceramics* 106 (6) (2007) 294–301.
- [62] R. Taylor, I.G. Richardson, R.M.D. Brydson, Composition and microstructure of 20-year-old ordinary Portland cement-ground granulated blast-furnace slag blends containing 0 to 100% slag, *Cement and Concrete Research* 40 (7) (2010) 971–983.
- [63] T.C. Powers, Physical properties of cement paste, *Proceedings of the Fourth International Symposium on the Chemistry of Cement*, session V, paper, V-1, 1960, pp. 577–613.
- [64] S. Gauffinet, et al., Direct observation of the growth silicate hydrate on alite and silica surfaces by atomic force microscopy, *Earth and Planetary Sciences* 327 (1998) 231–236.
- [65] A. Nonat, The structure and stoichiometry of C–S–H, *Cement and Concrete Research* 34 (9) (2004) 1521–1528.
- [66] J.J. Thomas, H.M. Jennings, A colloidal interpretation of chemical aging of the C–S–H gel and its effects on the properties of cement paste, *Cement And Concrete Research* 36 (1) (2006) 30–38.
- [67] H.M. Jennings, Refinements to colloid model of C–S–H in cement: CM-II, *Cement And Concrete Research* 38 (3) (2008) 275–289.
- [68] G. Constantinides, F.J. Ulm, The nanogranular nature of C–S–H, *Journal Of The Mechanics And Physics Of Solids* 55 (1) (2007) 64–90.
- [69] A.J. Allen, J.J. Thomas, H.M. Jennings, Composition and density of nanoscale calcium–silicate–hydrate in cement, *Nature Materials* 6 (4) (2007) 311–316.
- [70] J.P. Korb, L. Monteilhet, P.J. McDonald, J. Mitchell, Microstructure and texture of hydrated cement-based materials: a proton field cycling relaxometry approach, *Cement and Concrete Research* 37 (2007) 295–302.
- [71] P.J. McDonald, J. Mitchell, M. Mulheron, J.P. Korb, Two-dimensional correlation relaxation studies of cement, *Magnetic Resonance Imaging* 25 (4) (2007) 470–473.
- [72] L. Monteilhet, J.P. Korb, J. Mitchell, P.J. McDonald, Observation of exchange of micropore water in cement pastes by two-dimensional T-2–T-2 nuclear magnetic resonance relaxometry, *Physical Review E* 74 (6) (2006) 061404.
- [73] P.J. McDonald, V. Rodin, A. Valori, Characterisation of intra- and inter-C–S–H gel pore water in white cement based on an analysis of NMR signal amplitudes as a function of water content, *Cement and Concrete Research* 40 (12) (2010) 1656–1663.
- [74] Valori, A. Characterisation of cementitious materials by 1H NMR, PhD Thesis, University of Surrey, 2009.
- [75] R.J.M. Pelleng, A. Kushima, R. Shahsavari, K.J. Van Vliet, M.J. Buehler, S. Yip, F.J. Ulm, Realistic molecular model of cement hydrates, *Proceedings of the National Academy of Sciences of the United States of America* 106 (38) (2009) 16102–16107.